NUREG/CR-2649
SAND82-0752
R7
Printed May 1982

Influence of the Magnetomechanical Effect in Testing of Inductively Heated Ferritic Steel

Wendell B. Jones

Prepared by
Sandia National Laboratories
Albuquerque, New Mexico 87185 and Livermore, California 94550
for the United States Department of Energy
under Contract DE-AC04-76DP00789

Prepared for
U. S. NUCLEAR REGULATORY COMMISSION

Issued by Sandia National Laboratories, operated for the United States Department of Energy by Sandia Corporation.

Printed in the United States of America
Available from
National Technical Information Service
U.S. Department of Commerce
5285 Port Royal Road
Springfield, VA 22161

NTIS price codes
Printed copy: A03
Microfiche copy: A01

SAND820752

Influence Of The Magnetomechanical Effect In Testing Of Inductively Heated Ferritic Steel

Wendell B. Jones
Member, Technical Staff
Sandia National Laboratories
Albuquerque, New Mexico 87185

ABSTRACT

The use of a thermocouple spot welded to a specimen shoulder for temperature control in induction heated elevated temperature mechanical tests of ferritic alloys has been found inadequate to provide an unvarying temperature in the specimen gage. The magnetomechanical effect sufficiently alters the inductive coupling to produce both temperature cycling of +15K-50K and an overall cooling of 10K with mechanical cycling. These temperature changes can dominate the apparent strain measurements under conditions of limited plasticity.

INTRODUCTION

Several methods to heat metal specimens for elevated temperature mechanical testing are commonly used: conduction heating, radiant heating and induction heating. Induction heating is often used when the test apparatus is incompatible with bulky tube or clam-shell type furnaces. The convenience of producing high temperatures by using a simple small copper coil is offset by the difficulty in attaining and maintaining a constant temperature and a flat temperature profile. Often in testing it is desirable not to spot weld a thermocouple directly to the gage section of a specimen since this "flaw" would influence the failure. The alternative for temperature control is to spot weld a thermocouple to the specimen shoulder and use a dummy specimen with several spot welded thermocouples to determine appropriate controller set point is to get the desired gage temperature.

This procedure has been found to be inadequate in providing an unvarying test temperature for inductively heated ferritic steels during mechanical heating. The ferromagnetism of the 0.5 pct to 12 pct chromium ferritic steels of interest introduces the opportunity for several related magnetic effects to influence the temperature. Using the induction method, the specimen is heated by resistive eddy currents which are generated by the high frequency alternating current in the copper coil which surrounds it. The eddy current power consumption per unit surface area of a cylinder in a longitudinal field is:

$$p = \frac{H_m^2 (\mu \rho f)^{1/2}}{4\pi} \qquad (1)$$

where H_m is the amplitude of the field oscillating at frequency f, μ is the magnetic permeability and ρ is the electrical resistivity. The magnetic permeability of ferritic steels is large, about 600-1100 [2], and any experimental variable that influences the permeability would have a marked effect on the

power absorbed and, in turn, the temperature of the specimen. This is in contrast to the paramagnetic behavior of the austenitic stainless steels for which the permeability is about 1.008 and can be altered by only a few percent at most[3]. For the ferritic steels, the temperature of the specimen actually shows a stress dependence for both the permeability (magnetomechanical effect) and the resistivity (elastoresistance effect).[1]

Both the magnetomechanical and elastoresistive effects are manifestations of magnetostriction. Just as magnetizing an alloy can change its dimensions, straining a specimen can change its magnetization. Figure 1 shows the effect of stress on the permeability for a nickel alloy with positive magnetostriction similar to iron above 400°K.[1,3] The quantity $\lambda_s = \Delta\ell/\ell$, the saturation magnetostriction for polycrystalline iron is about $+10 \times 10^{-6}$ at typical elevated test temperatures of 800 to 900°K.[3,4] No data are available for the magnetostriction of dilute ferritic Fe-Cr alloys.

The electrical resistivity of a ferromagnetic alloy in a magnetic field is also influenced by stress. For alloys having positive magnetostriction, tensile stresses produce an increase in resistivity of a few percent and vice versa for compressive stresses.[1] While this effect is small, its influence on the eddy current power consumption is multiplicative with the magnetomechanical effect on μ which also increases due to tensile stress.

The exact influence these phenomena have on the gage temperature has not been determined analytically since the heat losses from the specimen cannot be calculated accurately. Instead, the overall effect has been measured in a mechanical test system under several conditions to characterize the temperature response.

EXPERIMENTAL MATERIALS AND TECHNIQUES

A straight sided cylindrical fatigue specimen of a Modified 9Cr - 1Mo ferritic steel* was used for quantitative measurements. Similar effects have been noted in both 2 1/4 Cr and 12 Cr ferritic steel specimens. The Curie temperature for all these alloys is between 1025 and 1075K[2], well above the test temperatures of 800 to 900K commonly encountered. The specimen was machined from a 25mm thick plate with the axis of the specimen transverse to the plate rolling direction. The plate was supplied in the normalized and tempered condition having a microstructure of fine, tempered martensite laths and fine carbide precipitates.

The specimen and induction heating coil arrangement used is typical of that in other laboratories[5]. The coil used here contains a reverse wound center loop to help eliminate any temperature peak at the center of the specimen. Most of the results described here were gathered with a control thermocouple welded to the shoulder and a thermocouples spot recording thermocouple welded to the gage section. It should be noted that temperature control by neither of these thermocouples would result in a constant applied field amplitude during mechanical testing since the stress in the shoulder changes when the applied load changes just as the stress in the gage changes. The diameters of the shoulder and gage sections are 12.7mm and 6.4mm respectively and thus the stresses are always in the ratio of 1:4. It is this factor of 4 difference in stress between shoulder and gage which accounts for the observed variation in gage temperature during stressing while the controller maintains a constant shoulder temperature. All the temperature data reported here are from the thermocouples spot welded to the gage section.

*Composition: 8-9.5 pct Cr, 0.85-7.05 pct Mo, 0.08-0.12 pct C, 0.30-0.60 pct Mn, 0.20-0.50 pct S

RESULTS AND DISCUSSION

Small step changes in stress were used to characterize the magnetomechanical effect for this ferritic alloy in terms of a steady state relationship between elastic stress and gage temperature. The temperature of this test series was controlled from the shoulder. The stress was cycled between $\pm$150 MPa in steps of 12.5 MPa up to 75 MPa and 25 MPa up to 150 MPa; each step level was held for 2-4 minutes to allow for temperature stabilization. Figure 2 shows that the gage temperature varies +1°K, -5°K over this range of stresses. The slight hysteresis present indicates that 4 minutes was not sufficient to produce steady state. The asymmetry of the temperature response may be due to an intrinsic asymmetry in the magnetomechanical[1,3] effect together with a contribution from the presence of conductive and radiative cooling.

When the continuously cycling response in Figure 3 is examined, several effects are observed. Shown here are the temperature histories from stress controlled cycles of different cyclic periods (t_c). Also plotted are the data from Figure 2 representing the steady state response (labeled $t_c = \infty$). When the cycle time is decreased, the thermal mass of the specimen causes the magnitude of the temperature change to decrease and a phase shift between the stress and temperature cycles to occur. In addition, the biased nature of the magnetomechanical effect leads to an overall cooling trend in the gage temperature. Figure 4 shows that when t_c = 4s the gage temperature for this stress cycle reaches a steady state temperature about 1°K below the starting temperature. Shown for comparison is the gage temperature when that is the thermocouple used for temperature control.

Strain measurements are greatly complicated by these changes in temperature since the diameter (or gage length) measured by the extensometer reflects dimensional changes due both to stress and thermal expansion. The

measured change in diameter (δ) can be written as:

$$\frac{\delta}{d_o} = \alpha\Delta T + \varepsilon_d \qquad (2)$$

where d_o is the unstressed diameter at the starting temperature, ΔT is the stress dependent change in temperature, α is the linear coefficient of thermal expansion, and ε_d is the mechanical diametral strain. The mechanical strain may include both elastic and inelastic parts according to:

$$\frac{\delta}{d_o} = \alpha\Delta T - \frac{\nu\sigma}{E} + \varepsilon_{pl} \qquad (3)$$

where ν is Poisson's ratio, ε is Young's modulus and ε_{pl} is the diametral plastic strain.

In order to examine quantitatively the effect of temperature changes on the measured strains (δ/do), several tests were conducted at 700K to eliminate the inelastic strains present in the data taken at 866K shown in Figures 2 through 4. The axial mechanical strain can then be given as:

$$\varepsilon = \frac{1}{\nu}\left(\alpha\Delta T - \frac{\delta}{d_o}\right) \qquad (4)$$

A series of steploading cycles at 700K produced the apparent stress/strain response shown in Figure 5. Using the temperature correction in Equation 4 these data are found to fall very close to the anticipated purely elastic ($\varepsilon = \sigma/E$) mechanical response. A comparison of the corrected and uncorrected data shows that the temperature change ($\alpha\Delta T$) contribution to the measured strain can be larger than the elastic strain alone. The success of the correction in Figure 7 also confirms the validity of the thermocouple measurements.

Since the ($\alpha\Delta T$) term can be substantial compared to the mechanical strain, there can be large differences in the strains inferred from diameter and axial strain measurement. The differences arise since an increase in

temperature will produce an increase in axially measured strain, whereas the same increase in temperature will also produce an increase in the diameter which would be interpreted as a decrease in axial strain when using diametral extensometry. Using the data from Figure 5, axial strain has been calculated in several different ways. First, the axial strain that would be measured by an axial extensometer was evalulated according to:

$$\varepsilon = \frac{\sigma}{E} + \alpha\Delta T \tag{5}$$

This behavior is compared to the axial strain as calculated from the diametral extensometer measurements:

$$\varepsilon = -\frac{1}{\nu}\varepsilon_d = \frac{\sigma}{E} - \frac{\alpha\Delta T}{\nu} \tag{6}$$

This difference in both sign and magnitude of the temperature correction is shown in Figure 6 and illustrates that both the temperature control scheme and the type of extensometer used must be considered to properly correct strain measurements when an uncompensated magnetomechanical effect has been present.

CONCLUSIONS

1. The magnetomechanical effect alters the magnetic permeability of ferritic steels under stress to an extent sufficient to influence the inductive heating characteristics. When the temperature of the specimen shoulder is used for control at 866K, the gage temperature was found to cycle between 816K and 881K when stress was slowly cycled between ±150 MPa.

2. As the period of cycling was shortened from 20 minutes to 4s, the dominant effect shifted from temperature cycling to an overall cooling of the gage to about 853K.

3. In many cases the apparent strain was dominated by temperature induced diameter change. When this effect was subtracted from the apparent strain measurements, all the hysteresis and mean strain effects were removed.

REFERENCES

1. Bozorth, R. M., Ferromagnetism, D. Van Nostrand Co. Inc., New York (1951).

2. Peckner, D. and Bernstein, I. M., Handbook of Stainless Steels, McGraw-Hill Book Co., New York (1977).

3. Cullity, B. D., Introduction to Magnetic Materials, Addison-Wesley Publishing Co., Reading, Mass. (1972).

4. Tatsumoto, E. and Okamoto, T., "Temperature Dependence of the Magnetostriction Constants in Iron and Silicon Iron," J. Phys. Soc. Japan, 14(3), 1583-1594 (1959).

5. Slot, T., Stentz, R. H., and Berling, J. T., "Controlled-Strain Testing Procedures," in Manual On Low Cycle Fatigue Testing, ASTM STP 465, Philadelphia, PA (1969).

CAPTIONS TO FIGURES

Fig. 1 Effect of tensile stress on the maximum permeability (positive magnetostriction). From Bozorth[1].

Fig. 2 Steady state temperature changes resulting from small steps in applied load when the shoulder temperature is held constant.

Fig. 3 Temperature variation produced from stress controlled cycling at several different periods.

Fig. 4 Temperature change during 70 cycles at a 4s period.

Fig. 5 Comparison of the measured apparent strain with the calculated pure mechanical strained in the same cycles.

Fig. 6 The steady state cyclic response from Figure 2 shown as pure mechanical strain and apparent axial strain calculated by two methods (see text).

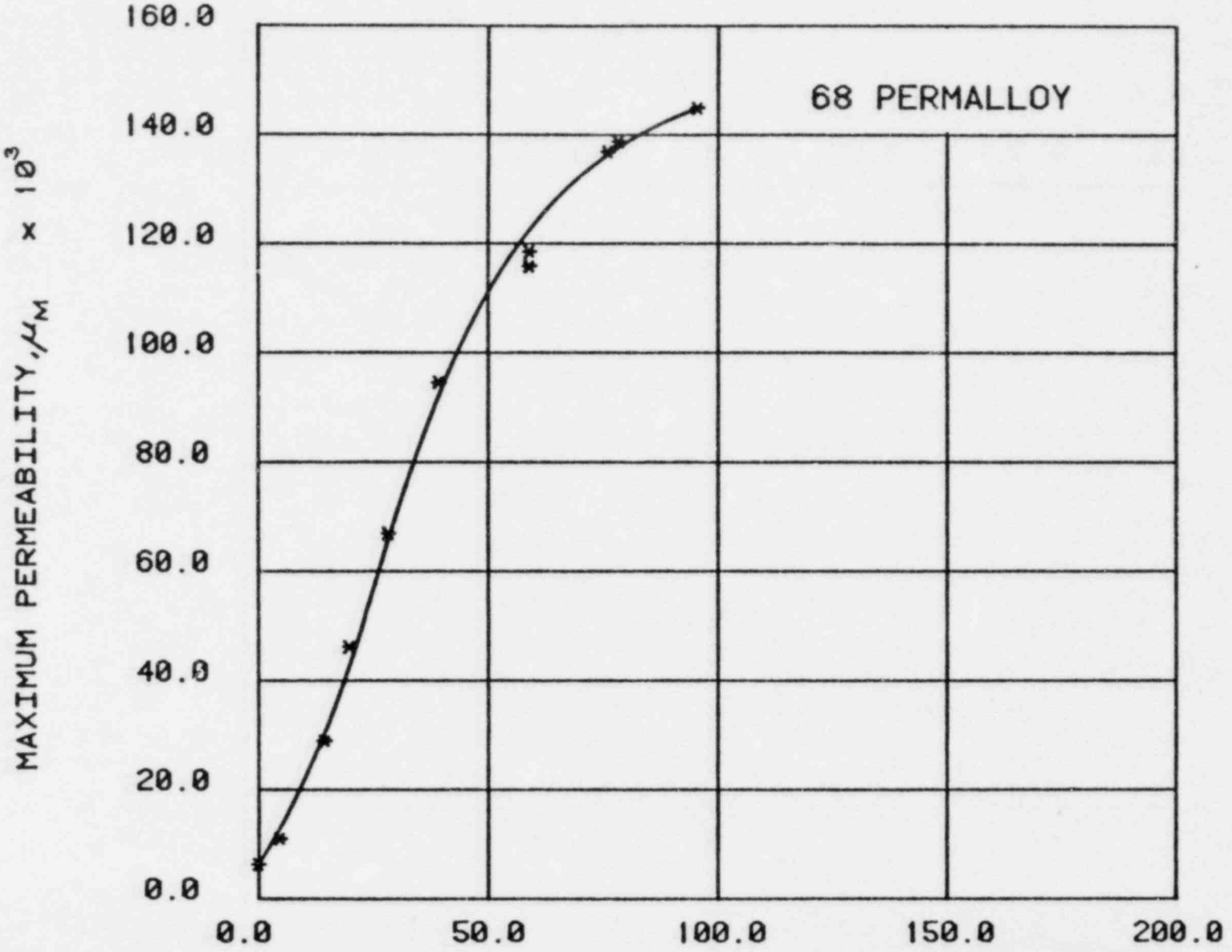
68 PERMALLOY
MAXIMUM PERMEABILITY, μ_M x 10^3
160.0
140.0
120.0
100.0
80.0
60.0
40.0
20.0
0.0
0.0
50.0
100.0
150.0
200.0
STRESS, σ IN MPa

FIGURE 1

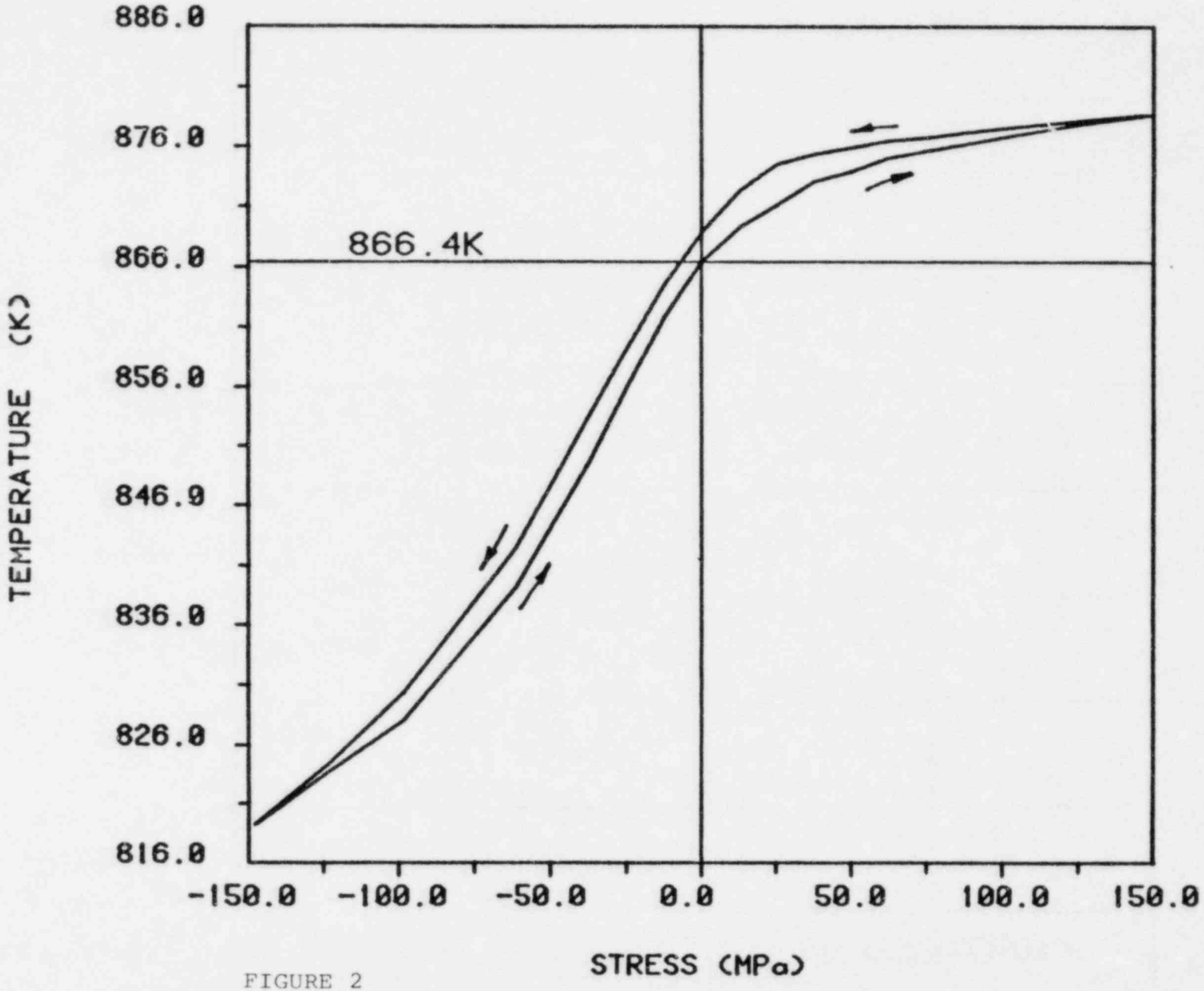
886.0
876.0
866.0
856.0
846.9
836.0
826.0
816.0
866.4K
TEMPERATURE (K)
-150.0
-100.0
-50.0
0.0
50.0
100.0
150.0
STRESS (MPa)

FIGURE 2

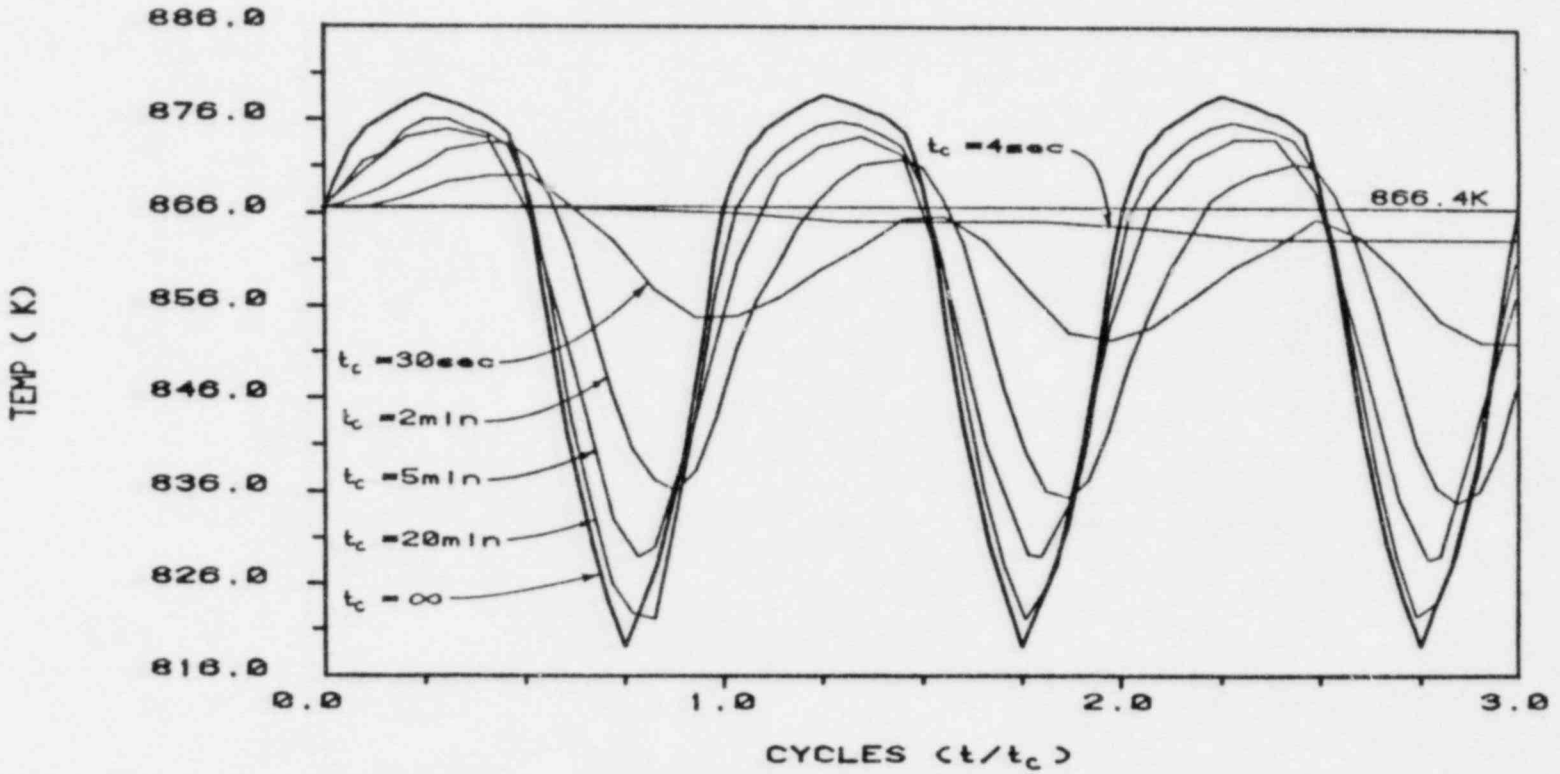
886.0
876.0
866.0
856.0
846.0
836.0
826.0
816.0
TEMP (K)
0.0
1.0
2.0
3.0
CYCLES (t/tc)
tc =4sec
866.4K
tc =30sec
tc =2min
tc =5min
tc =20min
tc =∞

FIGURE 3

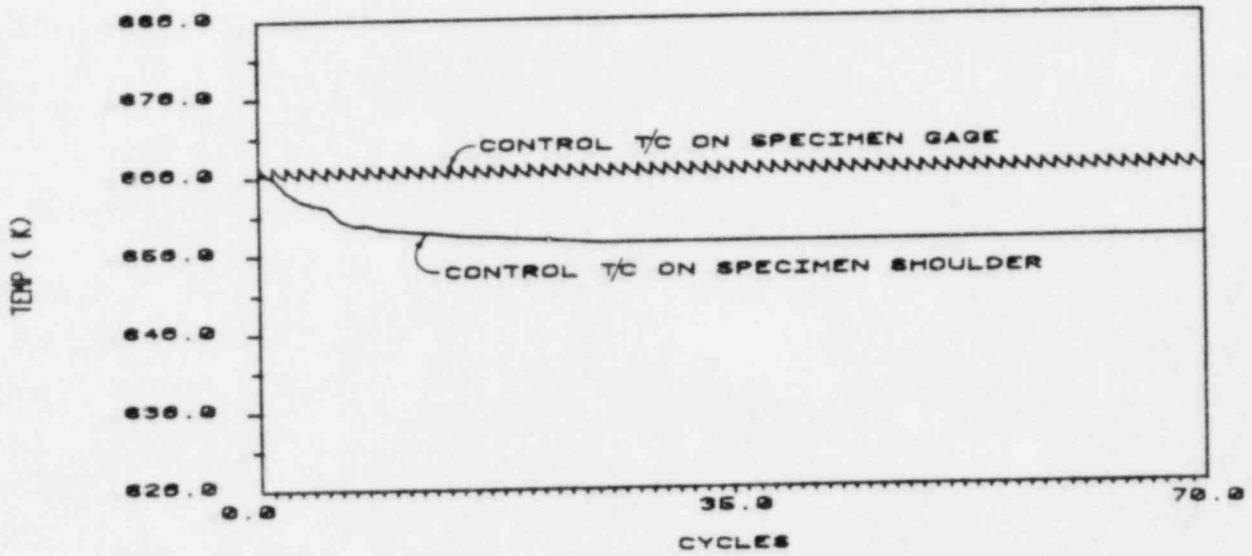
680.0
670.0
660.0
650.0
640.0
630.0
620.0
TEMP (K)
CONTROL T/C ON SPECIMEN GAGE
CONTROL T/C ON SPECIMEN SHOULDER
0.0
35.0
70.0
CYCLES

FIGURE 4

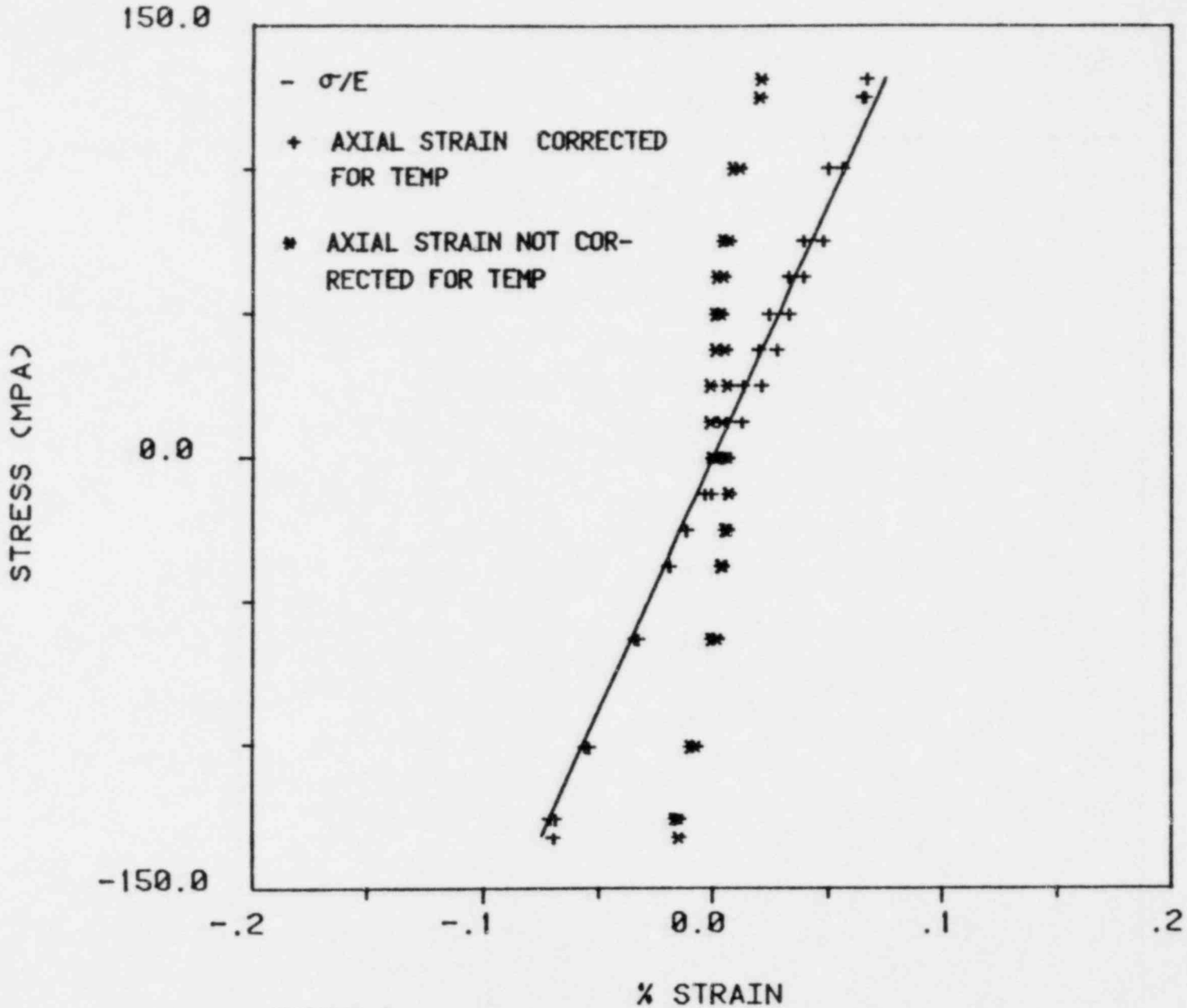
150.0
0.0
-150.0
STRESS (MPA)
- σ/E
+ AXIAL STRAIN CORRECTED FOR TEMP
* AXIAL STRAIN NOT CORRECTED FOR TEMP
-.2
-.1
0.0
.1
.2
% STRAIN

FIGURE 5

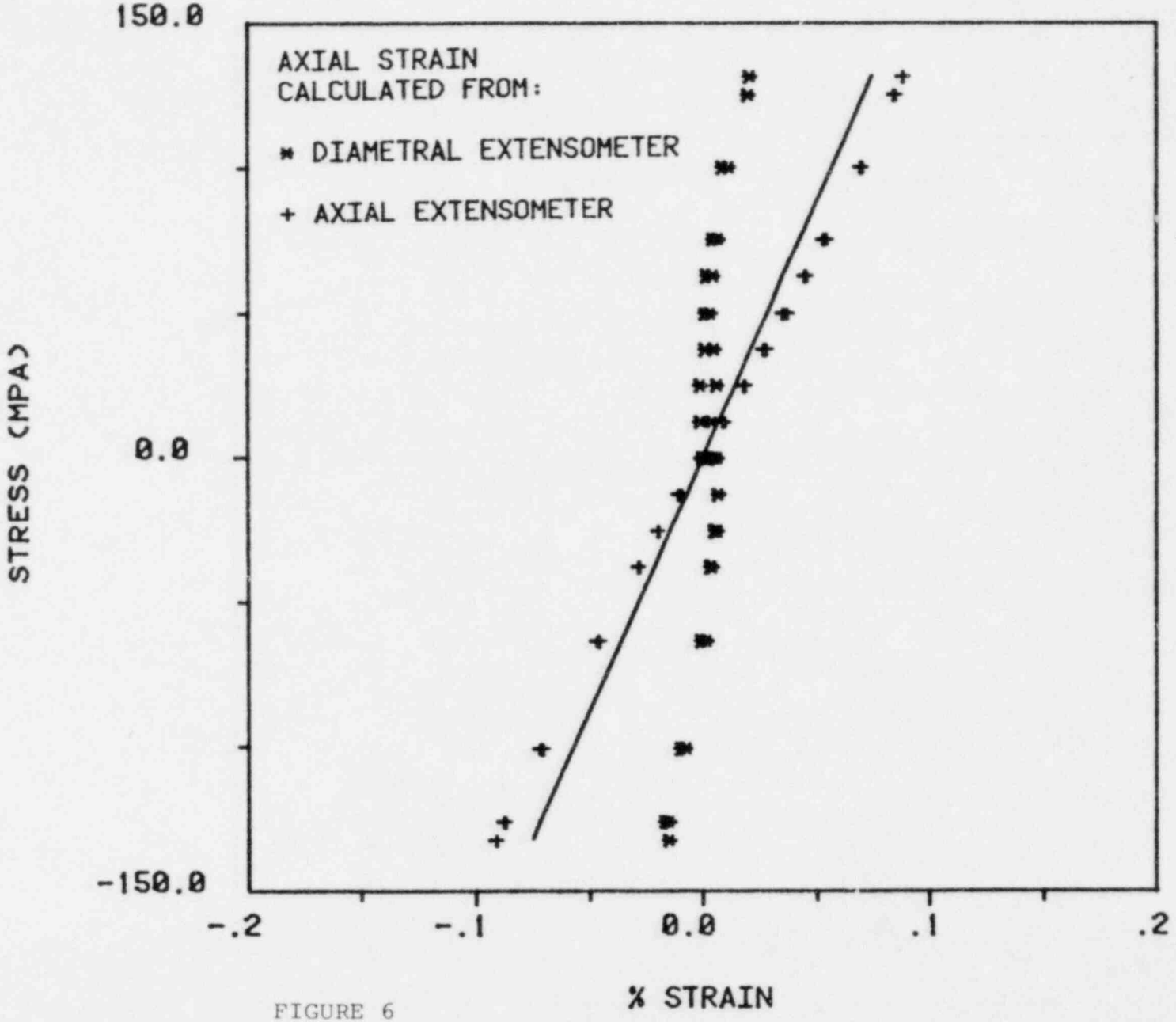
150.0
0.0
-150.0
STRESS (MPA)
AXIAL STRAIN
CALCULATED FROM:
* DIAMETRAL EXTENSOMETER
+ AXIAL EXTENSOMETER
-.2
-.1
0.0
.1
.2
% STRAIN

FIGURE 6

Distribution:

U. S. Nuclear Regulatory Commission
(380 copies for R7)
Division of Document Control
Distribution Services Branch
7920 Norfolk Avenue
Bethesda, MD 20014

U. S. Nuclear Regulatory Commission (54)
Division of Reactor Safety Research
Office of Nuclear Regulatory Research
Washington, DC 20555
Attn: C. N. Kelber, Assistant Director,
Advanced Reactor Safety Research
R. T. Curtis, Chief
Analytical Advanced Reactor Safety Research, ARSR
T. J. Walker (50)
M. Silberberg, Chief
Experimental Fast Reactor Safety

U. S. Department of Energy
Office of Nuclear Safety Coordination
Washington, DC 20545
Attn: R. W. Barber

U. S. Department of Energy (2)
Albuquerque Operations Office
P. O. Box 5400
Albuquerque, NM 87185
Attn: J. R. Roeder, Director
Operational Safety Division
D. K. Nowlin, Director
Special Programs Division
For: C. B. Quinn
D. Plymale

B. C. Wei
Division of Reactor Development and Demonstration
Department of Energy
Mail Stop F-309
Washington, DC 20545

W. O. Harms (5)
Materials and Structures Technology Management Center
Oak Ridge National Laboratory
Oak Ridge, TN 37830

T. Belytschko
Dept. of Civil Engineering
Northwestern University
Evanston, IL 60201

John Henry Associates, Inc. (2)
60 Hickory Drive
Waltham, MA 02154
Attn: T. Branca
T. Slot

J. A. Flaherty
Teledyne Materials Research Co.
303 Bear Hill Road
Waltham, MA 02154

C. R. Brinkman (4)
Metals and Ceramics Division
Oak Ridge National Laboratory
P.O. Box X
Oak Ridge, TN 37830
Attn: V. K. Sikka
J. P. Strizak
M. R. Booker

R. J. Slember
Westinghouse Electric Corp.
Advanced Reactors Division
Clinch River Site
P. O. Box W
Oak Ridge, TN 37830

Reactor Division (4)
Oak Ridge National Laboratory
P. O. Box "Y"
Oak Ridge, TN 37830
Attn: J. M. Corum
C. E. Pugh
R. Huddleston

R. D. Campbell
Engineering Decision Analysis Co.
2400 Michelson Drive
Irvine, CA 92715

C. Chan
Nuclear Safety and Analysis Prog.
Electric Power Research Institute
P. O. Box 10412
Palo Alto, CA 94304

M. Reich
Brookhaven National Laboratory
Upton, NY 11973

C. C. Schultz
The Babcock & Wilcox Company
Research & Development Center
P. O. Box 835
Alliance, OH 44601

I. Berman
Foster Wheeler Corporation
12 Peach Tree Hill Road
Livingston, NJ 07039

Foster Wheeler Corporation (2)
110 South Orange Avenue
Livingston, NJ 07039
Attn: D. H. Pai
J. M. Chern

T. Airman
Dept. of Aerospace & Mechanical Engineering
Notre Dame, IN 46556

Hanford Engineering Development Laboratory (2)
P.O. Box 1970
Richland, WA 99252
Attn: M. J. Anderson
L. K. Severud

Combustion Engr., Inc. (2)
1000 Prospect Hill Road
Windsor, CT 06095
Attn: R. Barsoum
C. W. Lawton

General Electric Company (2)
175 Curtner Avenue
San Jose, CA 95125
Attn: J. F. Copeland, M/C 513
Y. R. Rashid, M/C 138

J. B. Conway
Mar-Test Incorporated
45 Novner Drive
Cincinnati, OH 45215

A. W. Dalcher
Advanced Technology Department
General Electric Company
310 Deguigne Drive
Sunnyvale, CA 94086

Argonne National Laboratory (4)
9700 South Cass Avenue
Argonne, IL 60439
Attn: S. H. Fistedis
S. Majumdar
J. M. Kennedy

H. D. Hibbitt
MARC Analysis Research Corp.
105 Medway Street
Providence, RI 02906

J. Houstrup
Combustion Engineering Inc.
911 W. Main Street
Chattanooga, TN 37402

General Atomic Company (3)
P. O. Box 81608
San Diego, CA 92138
Attn: M. T. Jakub
D. I. Roberts
C. E. Washington

Rockwell International (2)
Atomics International Division
8900 De Soto Avenue
Canoga Park, CA 91304
Attn: H. M. Minami
R. I. Jetter

Harry Kraus
Rensselaer Polytechnic Institute
of Connecticut
275 Windsor Street
Hartford, CT 06120

E. Krempl
Dept. of Mechanical Enginering
Renssalaer Polytechnic Institute
Troy, NY 12181

M. Lemcoe
Battelle Memorial Institute
505 King Avenue
Columbus, OH 43201

M. J. Manjoine
Westinghouse Electric Corp.
Research and Development Center
1310 Beulah Road
Pittsburgh, PA 15235

S. S. Manson
Dept. of Mechanical Engineering
Case Western Reserve University
Cleveland, OH 44106

P. V. Marcal
MARC Analysis Research Corp.
314 Court House Plaza
260 Sheridan Avenue
Palo Alto, CA 94306

D. M. Norris
Lawrence Livermore Laboratory
P.O. Box 808
Livermore, CA 94550

W. J. O'Donnell
O'Donnell & Associates, Inc.
5100 Centre Avenue
Pittsburgh, PA 15232

E. P. Esztergar
6308 Avenida Cresta
La Jolla, CA 92037

J. R. Farr
Babcock & Wilcox Company
Power Generation Division
29 South Van Buren Avenue
Barberton, OH 44203

J. T. Fong
Applied Mathematics Division
National Bureau of Standards
Room A-302, Bldg. 101
Washington, DC 20234

J. C. Gerdeen
Dept. of Engineering Mechanics
Michigan Tech. University
Houghton, MI 49931

Westinghouse Electric Corp. (2)
Advanced Reactors Division
P. O. Box 158
Madison, PA 15663
Attn: D. S. Griffin
A. L. Snow

J. Hagstrom
Chicago Bridge & Iron Co.
800 Jorie Boulevard
Oak Brook, IL 60521

G. Halford
Mail Stop 49-1
NASA-Lewis Research Center
21000 Brook Park Road
Cleveland, OH 44135

1100 C. D. Broyles
Attn: J. D. Kennedy, 1110
T. L. Pace, 1120
G. L. Ogle, 1125

1537 N. R. Keltner
1537 R. U. Acton
1537 T. Y. Chu
2150 C. B. McCampbell
3434 B. N. Yates
4000 A. Narath
4231 J. H. Renken
4400 A. W. Snyder
4410 D. J. McCloskey
4420 J. V. Walker (5)
4421 R. L. Coats
4421 J. E. Gronager
4421 J. T. Hitchcock
4421 G. W. Mitchell
4421 C. Ottinger
4421 J. B. Rivard
4422 D. A. Power
4422 R. M. Elrick
4422 J. E. Smaardyk
4422 D. W. Varela
4423 P. S. Pickard
4423 A. C. Marshall
4423 D. A. McArthur
4423 K. O. Reil
4424 M. J. Clauser
4424 E. R. Copus
4424 E. F. Haskin
4424 P. J. McDaniel
4424 J. P. Odom
4424 F. W. Sciacca
4424 M. E. Senglaub
4424 D. C. Williams
4425 W. J. Camp
4425 E. Bergeron
4425 W. M. Breitung
4425 F. Briscoe
4425 R. J. Lipinski
4425 K. K. Murata
4425 M. L. Schwarz
4425 A. Soo-Anttila
4425 M. F. Young
4426 G. L. Cano
4426 J. G. Kelly
4426 H. L. Scott
4426 K. T. Stalker
4426 W. H. Sullivan
4426 S. A. Wright
4441 M. L. Corradini
4450 J. A. Reuscher
4451 T. R. Schmidt
4452 M. Aker
4723 D. O. Lee
5500 O. E. Jones
5530 W. Herrmann
5534 D. A. Benson
5541 W. Luth
5800 R. S. Claassen
5820 R. E. Whan
5822 K. H. Eckelmeyer
5830 M. J. Davis
5832 R. W. Rohde
5833 J. L. Jellison
5834 D. M. Mattox
5835 C. H. Karnes
5835 W. B. Jones (4)
5836 J. L. Ledman
5837 R. S. Blewer
5847 R. A. Sallach
5846 E. K. Beauchamp
8123 W. D. Zinke
8214 M. A. Pound
8310 D. M. Schuster
8314 A. J. West
8316 J. C. Swearengen
3141 L. J. Erickson (5)
3151 W. L. Garner (3)
For: DOE/TIC (Unlimited Release)
3154-3 R. P. Campbell (25)
For: NRC Distribution to NTIS

Org.	Bldg.	Name	Rec'd by	Org.	Bldg.	Name	Rec'd by

Sandia National Laboratories